

CHARACTERIZATION AND APPLICATION OF TAILORED HYBRID BLANKS

OZAN SINGAR¹, DOREL BANABIC²

Abstract. Unlike mechanical joining processes such as clinching or riveting the challenges in connecting steel and aluminum by the conventional welding method are, on one hand, the different physical characteristics such as density, melting temperature, electrical conductivity and thermal expansion. On the other hand due to high heat input, a thick and brittle intermetallic phase seam (IMP) develops in the welded seam. This strongly distinctive phase seam reduces the formability of the welding line and limits the realization in a technical application. Besides through several well known welding tests a new welding technique called Cold Metal Transfer welding (CMT) was introduced by Fronius (Wels, Austria) which lead to an IMP seam of a few micrometers. The main aim of this study is to determine the characterization of the CMT weld and to prove the feasibility to form an aluminum steel hybrid plate into demonstrator components. Results indicate that joining and forming of the aluminum-steel joints with a thickness of 0.8 mm-1.2 mm and 1.75mm-3.0 mm in a butt-joint configuration is possible. Furthermore formability tests revealed additional difficulties in the forming of steel combined with a non-hardenable aluminum.

Key words: Joining, Material, Tailor hybrid blanks.

1. INTRODUCTION

The scarcity of resources of fossil fuels and increasing environmental awareness of modern society lead to the fact that car manufactures are increasingly searching for alternative materials and manufacturing methods. For this reason lightweight metals such as aluminum combined with steel can be found increasingly in the car structure [1]. Nowadays, the concept of tailored blanks is divided in four sub-groups: tailor welded blanks, patchwork blanks, tailor rolled blanks and Tailor Heat Treated blanks [2]. The review in [2] presents the potentials of the technology and the availability for further scientific investigations.

While tailored welded blanks of steel are used in many different components of the body shell, tailored hybrid blank (THB) are still in the development phase.

¹ Daimler AG, Sindelfingen

² Technical University of Cluj-Napoca

Various welding processes, i.e. Friction Stir Welding (FSW) [3, 4], Laser Welding [5–8], Laser MIG Welding [9, 10], Non Vacuum Electron Beam Welding [11, 12] or BiMetal Welding [13] have been tested to combine aluminum with steel. Giera et. al. [3] examined the FSW process to join the material combinations DC04 (1 mm)/AW5182 (1.15 mm) and DC04 (1 mm)/AW6016-T4 (1 mm) in butt-joint configuration.

Nevertheless steel aluminum tailor welded blanks in a sheet thickness of about 1 mm are not feasible within the conventional FSW technology [4]. Further investigation of Giera [4] shows the enhancement of the weldability as well as the reduction of the wear of the tool by preheating the steel sheet near the joining zone. Tensile tests indicate tensile strength of up to 200 N/mm², which corresponds to about 80% of the tensile strength of unaffected aluminum base material. DC04 and the precipitation hardenable aluminum alloy AA6016-T4 in sheet thicknesses of about 1 mm achieved in the cup deep drawing experiments drawing ratio about 1.6.

Analysis proved neither with light microscopy nor with scanning electron microscopy the existence of intermetallic phases [4]. Seefeld et. al. [5–7] developed in his study a method to join aluminum with steel in lap joint configuration by using a Nd:YAG-laser. Microscopic test shows a homogenous connection with an IMP thickness between 2 μm–5 μm. All tensile test specimens failed in the HAZ of aluminum at maximum tensile strength of 192 N/mm².

Furthermore, the same principle was used to join AW6016-T4 1.15 mm with DC05 ZE75/75 0.8 mm in butt-joint configuration with an AlSi12 filler material. Tests represent IMP under 2 μm and a maximum tensile strength of 188 N/mm². In addition, Radscheit [8] examined the lap joint shear strength of a St12 1mm/AW6061-T4 1mm combination welded by two different Nd:YAG-laser sources. Intermetallic phases with a thickness of up to 57 μm occur between the different material by using a 350 W Laser and a welding speed of 0.75 mm/s.

However, further welding tests indicates a reduction of the IMP-thickness to 10 μm by increasing the welding speed to 15 mm/s and using a 1500 W Laser. Kreimeyer and Vollersten present in [9] that using a hybrid process (Nd:YAG-laser +MIG), a gap tolerant joining of aluminum-steel joints with a thickness of 3mm–4mm, in butt-joint configuration is possible. Joints were realized with small intermetallic phase layers in form of Al₅Fe₂ and Al₃Fe (phase seam thickness below 10 μm). The static tests revealed that the gap has an influence on the strength of the joints. For a zero gap a static strength of approx. 100 N/mm² was reached. In comparison, the samples joined with a 1 mm gap reaches only 40% of the static strength. A hydromechanical deep drawing test in [10] was achieved by applying a pressure of 65 bar. Aside from some slight transverse cracks in the weld metal in the zone of the edge radius of the plate, no defects were observed. Another joining technique to combine aluminum with steel was developed by Lau [11]. Lau examined the IMP, tensile strength and formability of the connections in butt/lab-joint configuration joined by the NonVacuumElectronBeam Welding technology.

The highest IMP thickness occurs up to 20 μm. The maximum tensile stress achieved with a butt-joint configuration by a tensile stress of 355 N/mm².

In all configurations deep drawing ratio of 1.6 and 1.9 could not be realized. Further investigations from Bach et. al. can be found in [12]. In [13] it is introduced the BiMetal Welding. Results present IMP thicknesses of 0.5 mm and a tensile strength of 125 N/mm². Singar et al. [14] determined in first fundamental experiments mechanical properties of a CMT weld.

Tensile tests with online deformation analyses show that the main formation takes place on the aluminum side. Another conclusion of this study is that the weld line has the tendency to move during the forming operation toward the direction of the steel. All specimens failed in the ductile material aluminum. In this regard, weld line displacement is an important indicator of deformation and caution should be taken for designing THBs forming operations. Furthermore, a numerical simulation model of the CMT weld has been carried out in [1]. In the present paper, the application of the hybrid blanks welded by CMT technology is presented.

2. CMT WELDING

In this study welded aluminum and steel THB were made available for the investigations in cooperation with the two companies voestalpine & Fronius. The plates are arranged using a special die type where the steel sheet is sharpened using a rolling process and a notch is made in the aluminum. As shown in Fig. 1, the welding system is equipped with two torches which join the sheets in an oscillating movement of the filler wire from both sides.

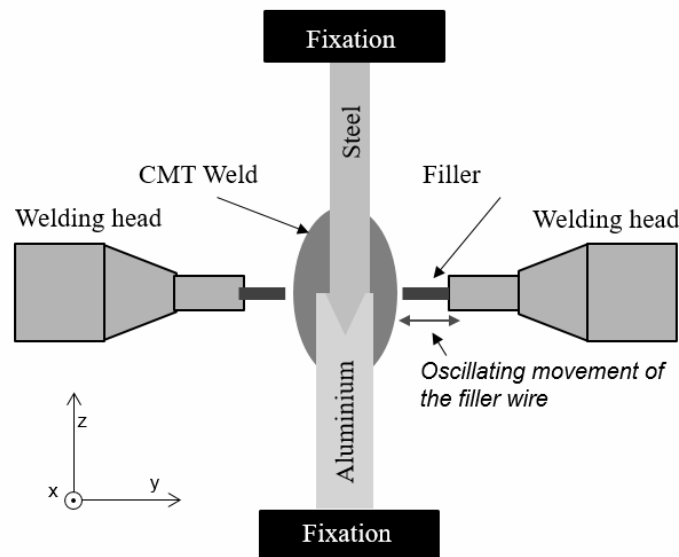


Fig. 1 – Welding process.

The selection of basic parameter settings for CMT soldering is based on the knowledge of the two companies. The feed is adjusted by the negative movement of the clamping technology in the x direction at a constant speed of $V_f = 80 \text{ cm/min}$. Other joining parameters such as wire feed with $V_w = 4.5 \text{ m/min}$, current with $I = 70 \text{ A}$, voltage with $U = 12 \text{ V}$ and oscillation frequency with $f = 70 \text{ Hz}$ were also kept constant during joining. Overall, the joining tool, which is still considered as a prototype, can be used to manufacture THB plates with a maximum welding length of up to approx. 600 mm. A description of the welding procedure is shown in Fig. 2a. In addition all test specimens has the special patented butt joined geometry from voestalpine with its characteristic wedged steel plate end [14] – Fig. 2b.

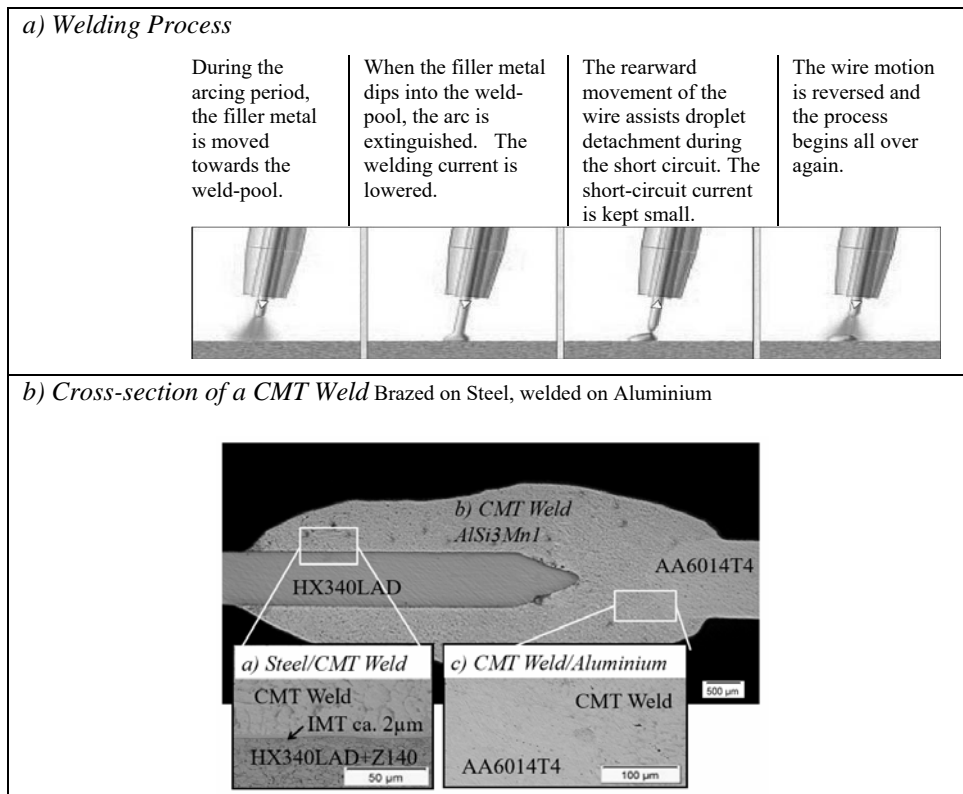


Fig. 2 – Schematic CMT Welding. a)Welding Procedure; b) cross section.

The mechanical properties of the used basic materials and the filler AlSi3Mn1 are listed in Table 1. The base materials qualities were determined by means of tensile test at room temperature. The schematic of the CMT-welding technique can be found in [14]. Galvanized steel blank sheets HC340LAD were

combined with aluminum alloys AA6016-T4 and AW5182. To avoid a distortion the samples were clamped during the process. The weld line has two characteristic compounds, welded on the aluminum plate and brazed on the steel side. The requirement for brazing connection on steel plate is a zinc coat layer on both sides. In addition, all test specimens have the special patented butt-joined geometry from voestalpine [15, 16].

Table 1

Base materials and filler wire

Material		Zinc layer [μm]	YS [MPa]	TS [MPa]	UE [%]	E [MPa]	n [-]
HC340LA	Base Material	9.9	383.64	457.89	15.24	211920.12	0.15
AA6014T4	Base Material		138.71	228.39	20.48	68147.44	0.23
AW5182	Base Material		110	255	13	71000	-
AlSi ₃ Mn ₁ acc. [16]	Filler wire		50	120	25		-

3. MECHANICAL CHARACTERIZATION OF THE WELDED MATERIALS

To characterize the mechanical properties of the THB connection, the combination of uniaxial tensile and microhardness tests is used in this work. First and foremost the sufficient manufacturing quality of the weld seam should be illustrated by uniaxial tensile tests across the weld seam. The hardness measurement is used to determine the lateral expansion of the heat affected zone caused by the CMT welding process.

3.1. UNIAXIAL TENSILE TEST

The uniaxial tensile test perpendicular to the weld seam is used to investigate the strength behavior of the weld seam when it is arranged transversely to the load direction. Figure 3 shows the tensile force over the deformation for the material combination HC340LA 0.8 mm/AA6014 used. The failure occurs in five measured samples without exception in the aluminum base material. The crack runs parallel to the weld at a distance of about 30 mm from the center of the weld and achieves a tensile strength of about 93% of the aluminum base material. Compared to the tensile test of the pure aluminum base material, with the same sample geometry and constant sheet thickness of 1.2 mm, due to the sheet thickness differences

$t_{\text{Steel}} \neq t_{\text{Aluminum}}$, as well as the unequal material distribution on the THB sample (50% aluminum/50% steel), the total stretch reach a max of 68%. Assessing the results shows that the weld seam strength is not affected by the weld irregularities such as pores, cracks, edge notches or seam bulges. The tensile strength almost corresponds with the less strong aluminum base material. Apart from the aluminum base material, the load-bearing cross-section of the weld seam is the most important factor influencing the static strength of the connection. Table 4 shows the geometrical dimensions of the sample after the tensile test. The thickness of the CMT seam remains constant compared to the original initial state with $d_{\text{max}} = 3.02 \text{ mm}$ (standard deviation: 0.058). In the tensile test perpendicular to the weld seam the force-displacement curves provide minor information about the elongation value of the entire sample. There is no statement about the actual expansion proportions in the area of the weld seam or in the base materials.

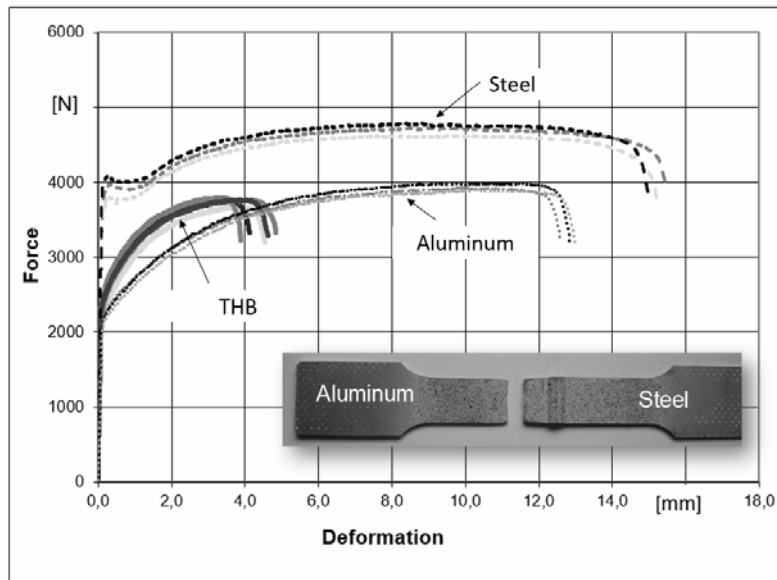


Fig. 3 – Force-Displacement distribution of a transversely arranged CMT weld in tensile tests for material HC340LA 0.8 mm/AA6014 1.2 mm.

Despite of mechanical analyses local deformation was measured online during the test. The measurement was carried out by means of the optical measurement system ARAMIS. A stochastic pattern was sprayed by using graphite on the surface of the specimen. The cam measures the changes in deformation in longitudinal ε_x and transversal ε_y direction of the measuring grid and provides the data for the calculation, Fig. 4 represent the output data in longitudinal (main deformation ε_x direction). Up to a slight stretch of approx. 0.0045, there is an

almost even distribution of stretch in the area of the CMT seam and the base materials. From this point, a clear plastic stretch can be seen in the aluminum area.

With a maximum local elongation of more than 0.35 the constriction begins parallel to the weld seam with the result that the sample ultimately fails. Due to the material and thickness ratio between steel or CMT seam and aluminum no significant plasticization is recorded in the steel sheet and in the area of the CMT seam.

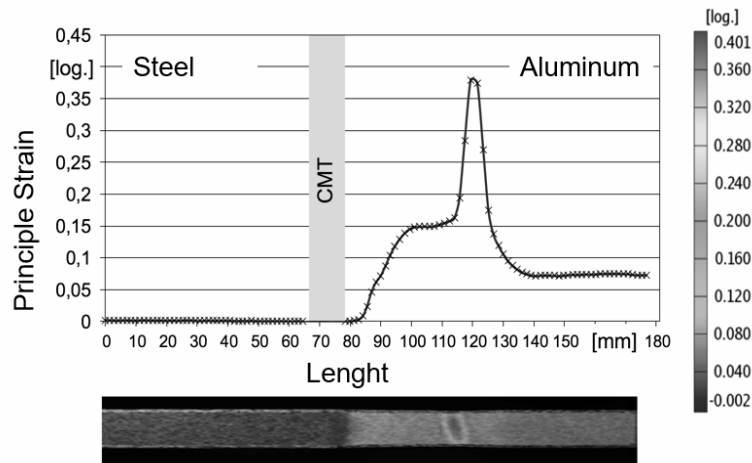


Fig. 4 – Strain distribution of a transversely arranged CMT weld in a tensile test.

Table 2

Geometric dimensions after the tensile test

Sample	Thickness [mm]			Width [mm]		
	Steel	Aluminium	CMT	Steel	Aluminium	CMT
1	0,789	1,151	3,092	13,836	13,663	13,811
2	0,783	1,164	2,975	13,922	13,808	13,959
3	0,778	1,151	3,090	14,031	13,949	14,035
4	0,780	1,171	2,948	14,003	13,960	14,036
5	0,781	1,180	3,019	13,971	13,909	14,010
Average	0,780	1,163	3,0248	13,952	13,857	13,970
Standarddeviation	0,0017	0,011	0,0586	0,0686	0,1121	0,0844

3.2. MICROHARDNESS TESTING

To determine the mechanical properties of the structural transformation caused by the CMT welding process and to determine the lateral extent of the heat-affected zone (HAZ) in the area of the joint connection, the instrumented penetration test according to Vickers is carried out. Figure 5 shows the course of the Vickers hardness HV0.1 across the weld seam and starting from the central plane of the sheet using the example of material HX340 LAD/AA6014. The calculated mean values and standard deviations of Vickers hardness HV0.1 refer to 67 individual measurements taken with a test force of 0.980 N on four different samples.

The distance between the individual measurement recordings was 0.31 mm within the series of measurements. Outside the weld area the initial hardness of the base materials was first determined.

A Vickers hardness of $HV_{0,1} = 180 \pm 19 \text{ N/mm}^2$ could be determined for the 0.8 mm thick steel material HX340LAD+Z140 (Fig. 5 area 1), while for the 1.2mm thick aluminum a value of $HV_{0,1} = 76 \pm 2 \text{ N/mm}^2$ (Fig. 5 area 5). With knowledge of the valid Vickers hardness of the base materials used it is now possible to carry out a quantitative analysis of the lateral expansion of the heat affected zone.

The hardness curve shows that the steel tip has a hardness peak of up to 270HV which is caused by the edge pretreatment by rolling, Fig. 5 area 2. In contrast there is a 5–7% softening compared to aluminum – recognize the base material in the thermomechanical influenced zone, Fig. 5 area 3. The softening of the 6xxx aluminum alloy in the weld seam is due to the fact that the precipitations of the Mg_2Si mixed crystal, which arise during the cold aging by the introduction of heat again can be undone.

A close look at the hardness values within the thermomechanical influenced zone of the measuring range 3–4 shows a high spread of the measured values. For this reason the distance from the steel tip from which the measured hardness profile deviates by at least twice the standard deviation from the hardener aluminum base material was used as the definition for the lateral expansion of the heat affected zone (HAZ). Taking into account the selected measurement resolution a HAZ zone of $b_{\text{HAZ}} = 1.1 \pm 0.1 \text{ mm}$ could be determined. The determination of the HAZ of the weld seam shows that the thermally influenced zone lies within the weld seam and shows no significant expansion in the direction of the aluminum base material.

Furthermore it was examined in the further course of the work whether there is a variation in the expansion of the thermally influenced zone in the direction of the seam thickness. For this purpose, the course of hardness perpendicular to the weld seam was determined at different intervals.

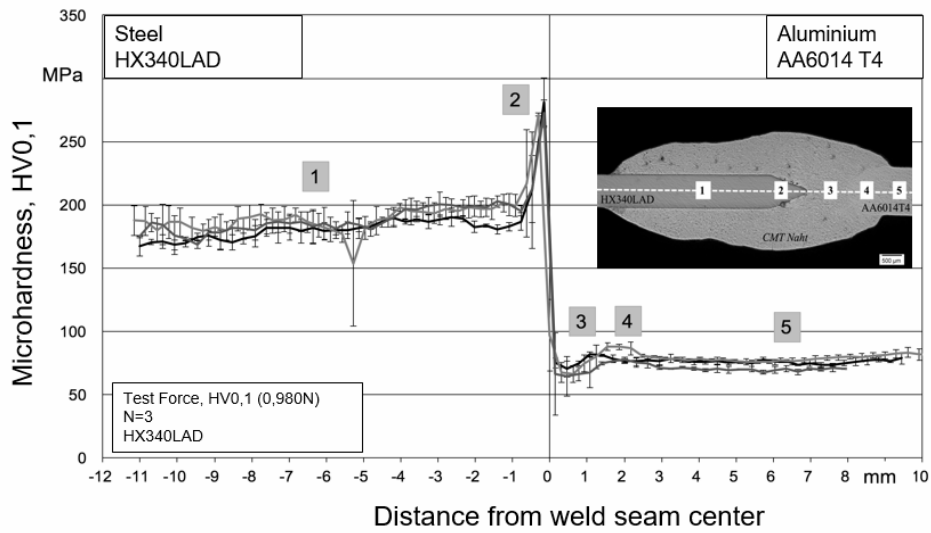


Fig. 5 – Microhardness curves.

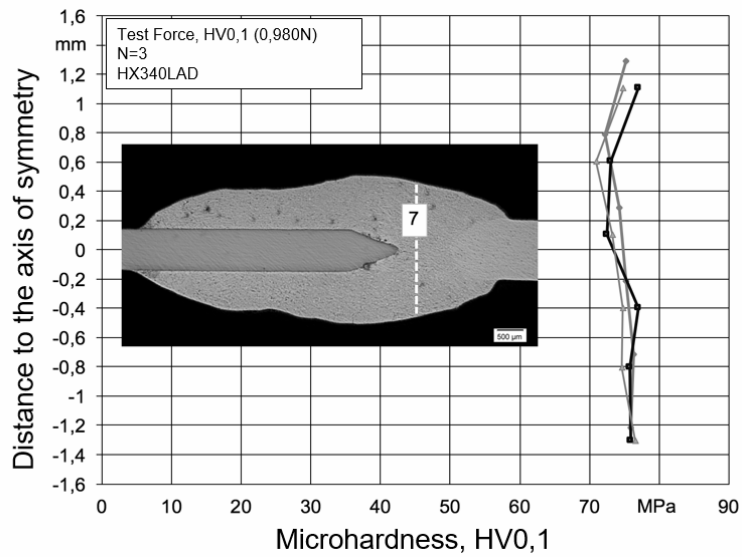


Fig. 6 – Microhardness curves across welding seam.

Using the same example of material combination, Fig. 6 shows the hardness curve for three different measurement series (area 7). Within the series of measurements three measuring points were recorded for top and bottom of the seam, starting from the central plane of the sheet. The course of hardness shows that there is no significant change in the hardness value in the direction of the seam thickness. The average hardness value is approx. $HV_{0,1} = 74.6 \pm 1.6 \text{ N/mm}^2$. The results show that constant mechanical properties in the seam thickness direction can be used with regard to the modeling of the CMT seam.

4. APPLICATION OF THB – PROTOTYPES AND TEST PREPARATION

Typical applications of steel tailored blanks in a body shell are for example door panels, side parts, wheel housing as well as longitudinal members. The basic idea behind the selection of prototypes for an aluminum steel component application is to consult large steel components in order to profit the advantage of the lightweight material. The joining sequence in the main productionline of the car body shell are usually due to accessibility not changeable (for example: main floor with sidewall), therefore a component of a sub-assembly group (for example: rear car) should be selected. Basically weight saving in the upper area (for example: roof) of the vehicle is more profitable than in the lower. This improves the driving behavior and agility of the car by moving the center of gravity down. Former corrosion tests showed that a seam sealing is necessary to protect the CMT weld line. Based on these results the prototype has to be in a non-visible area of the car body shell. The results of the Nakajima test obtained in [14] proved that the CMT laser weld restricts the deformation of the blank along the weld line.

The weld is deformed under plane strain conditions. The minor strain ε_2 in the forming limit diagram (FLD) along the weld is much smaller than the strain in zones more distant from the weld (in aluminum). Due to a greater material flow in aluminum, the weld line has the tendency to move during the forming operation toward the direction of steel. In this regard weld-line displacement is an important indicator of deformation and caution should be taken for designing forming operations. In general the decrease in forming limits arises mainly based on non-uniform deformation in the blank due to the difference in thickness, material properties, and also the presence of the weld bead. Therefore, forming geometry and the location of the weld has to be considered (weld line longitudinal to the bending axis). Due to the limitations of the welding process, the weld line has to be straight and no longer than approx. 600 mm.

Part screening on the areas frond end, rear end, roof and side wall of the body shell have been carried out under consideration of the above mentioned criterions. The presented example in Fig. 7a illustrates a roof frame which is assembled at the top of the car to the side wall by spot-welding. The part consists in the serial

process in microalloyed steel and has a thickness of 0.8 mm with a weight of 1.16kg. The unchanged microalloyed steel with a zinc coat layer of 9.9 μm has been combined with the aluminum alloys AA6016T4 and AW5182. The major advantage of this part is the simple formed geometry and the low deformation degree. The maximum bending radius lies at approx. 10 mm. The necessary tailored hybrid blank sheet is in total 1 200 mm length and 290 mm wide (aluminum 850 mm, 2 \times steel 175 mm). The calculated weight reduction with the current thickness and material combination brings in total – 0.48 kg (42%).

The second prototype represents Fig.7b. Basically the longitudinal member is used in the rear end and consists of two separate parts that are connected together by conventional welding method. The part is used in microalloyed steel HC340LA as well and has a thickness of 1.75 mm. The required hybrid blank for each part has a total length of 680 mm and a width of 320 mm (aluminum 550 mm, steel 130mm). The main challenge to create an aluminum steel hybrid component is on one hand the high thickness differences between steel and aluminum and on the other hand the enormous bending radius with approx. of max. 90°. To achieve a maximum weight saving by means of the highest possible proportion of aluminum, the CMT-weld line was placed far to the outside.

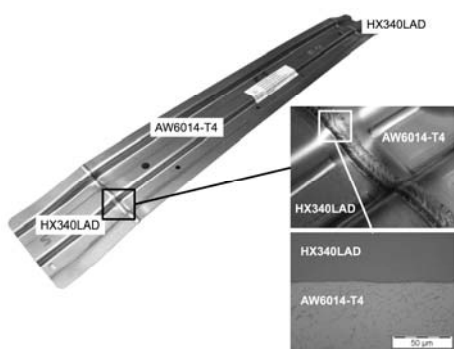
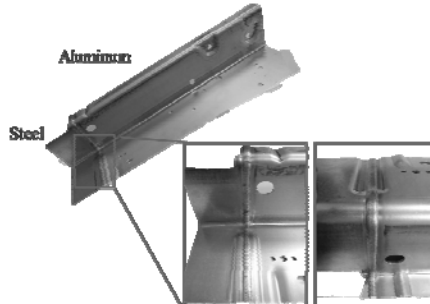
Prototype	Material combination 1	Material combination 2	TWB Blank [mm]	Thickness St/Al [mm]	Weld-seam width/length [mm]
Roof frame	HC340LA / AA6014-T4	HC340LA / AW5182	1200 / 290*	0.80 / 1.2	2.35 / 7.18
Longitudinal Member	HC340LA / AA6014-T4	-	680 / 320*	1.75 / 3.0	6.39 / 10.04
a) Roof frame			b) Longitudinal member		
					

Fig. 7 – Prototypes and Test preparation: a) roof frame; b) longitudinal member.

The necessary plates for the prototypes were welded by Fronius in Wels, Austria. Microscopic investigations were carried out in order to measure the weld width and length on each thickness combinations. According to the results grooves

milled out in the punch and in the die with respect to possible weld line movements, Fig. 8. Both prototypes were formed with a speed of $v = 45 \text{ mm/s}$ by using a Multidraw ALS40 (viscosity $420 \text{ mm}^2/\text{s}$ at 40°C) grease. The force was adjusted to $6\,000 \text{ kN}$ for the roof frame and $10\,000 \text{ kN}$ and for the longitudinal member.

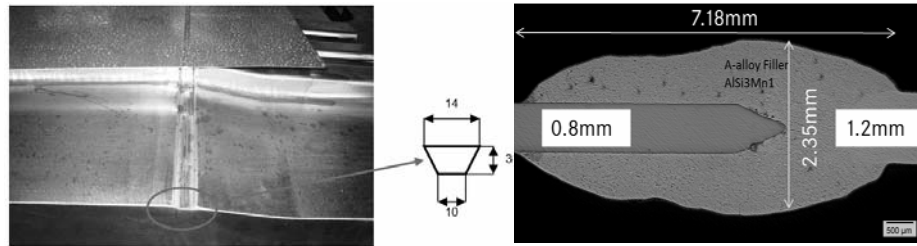


Fig. 8 – Adjusted Tool for the roof frame according to microscopic measurements.

5. RESULTS

Figures 7a and 7b show the formed prototypes with the material combination HC340LA/AA6014-T4. As can be seen neither the roof frame nor the longitudinal member indicates any defects on the CMT weld line after the forming operation. In addition, the weld line presents no weld line displacement into the direction of steel. A detailed examination has been carried out on the roof frame.

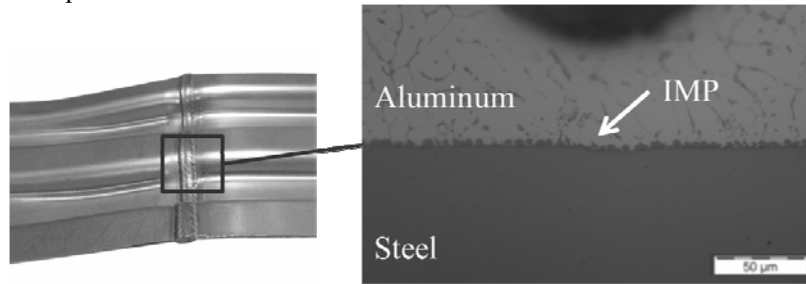
To prove the IMP – compound between steel and aluminum at the maximum bending radius, microscopic measurements performed. Results indicate no detection of the connection (Fig. 9a). By the modified thickness and material combinations spring-back effect is expected after the forming operation. Therefore, the deformed aluminum steel roof frame was measured with GOM ATOS in order to make a statement of shape changes compared to the serial steel component.

Usually the measurement system refers to the CAD-data set of the series parts. However due to the modified tools and expected influences, a steel roof frame was formed by means of the same adjusted tool and used as a reference. To avoid a light reflection the parts were sprayed with a water-based lime and mounted on rotatable console. The evaluation of the measurement is carried out by the software. The best-fit method sets the image of the aluminum steel roof frame over the reference steel part and sums the differences of the components reduced to the minimum. Local deviations can be accurately determined by means of individual cuts of this image. The maximum deviation lies in an acceptable range by $+2.78 \text{ mm}$ at the outer steel area and -1.97 mm in the aluminum referred to the standard steel part (Fig. 9b).

Last but not least a static compression test on the roof frame has been carried out. The roof frame cut out through the middle (in aluminum) and joint by a MIG-welding process to a quadratic aluminum plate. The steel side of the roof frame was also shorted to avoid a bending and increase the pressure on the weld line. Test results present no defects of the weld seam by applying force of up to 15 000 N (Fig. 10).

The roof frame was also combined with the non-hardenable alloy AW5182. The hybrid blank sheet shows no failures of the CMT weld. Nevertheless all the parts indicate defects on the CMT weld after the forming operation of the roof frame. It can be clearly seen that the weld bursts especially in the areas of multiaxial stress states. Fig. 11 left presents the weld line dissolved on the steel side by starting a crack on the maximum bending radius.

a) Microscopic measurement



b) GOM measurement

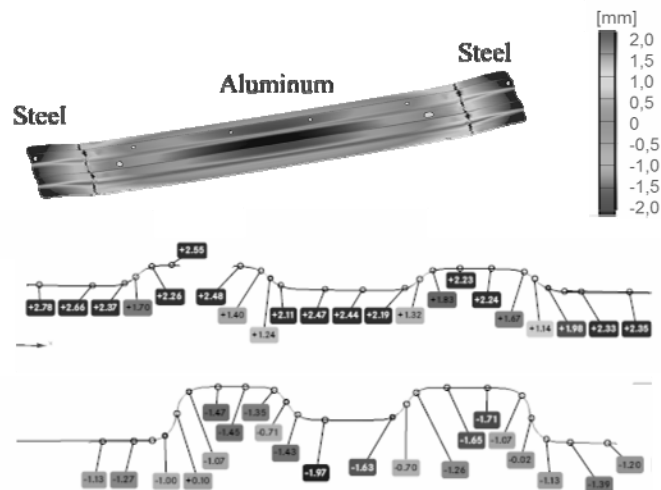


Fig. 9 – Roof frame examination: a) microscopic measurements; b) GOM measurement.

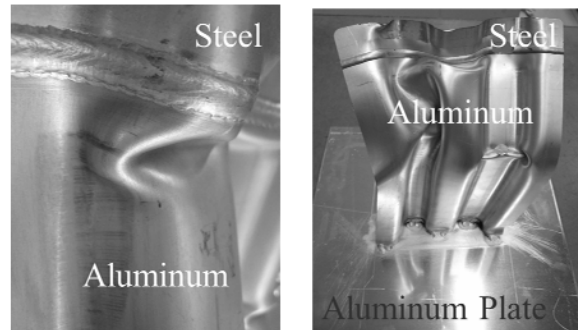


Fig. 10 – Compression test.

In addition a crack occurred transverse and along to the welding direction (Fig. 11 right). Magnesium is in the non-hardenable group 5××× of the main alloy with 4%–5%. However the reason for the cracks is due to the non-diffusion of Magnesium during the welding process.

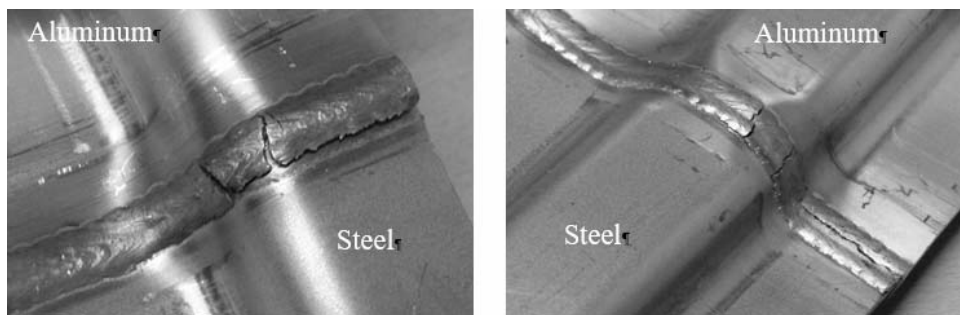


Fig. 11 – Material combination HC340LA/AW5182.

6. DETERMINATION OF LIGHTWEIGHT CONSTRUCTION COSTS

The additional lightweight construction costs are determined using Eq. (1). The equation consists of the quotient of manufacturing costs (HK) per weight saved (GW).

$$\text{LBMK} = \frac{\text{HK}_{\text{thb}} - \text{HK}_{\text{steel}}}{\text{GW}_{\text{thb}} - \text{GW}_{\text{steel}}} \left[\frac{\text{€}}{-\text{kg}} \right]. \quad (1)$$

The manufacturing costs of the THB (HK_{thb}) are calculated from the material costs of the plate, the manufacturing costs of the supplier and the internal pressing as well as the quotient of the use of funds and the total number of

components over the life cycle. Assuming an annual production quantity of 220,000 units, an LBMK (Lightweight Construction Cost) value of € 7.89/kg is calculated.

7. CONCLUSION

While tailored blanks made by steel or aluminum are already in series applications the hybrid tailored blanks are still in the development and testing phase. Compared to other welding techniques the CMT welding process allows a combination of aluminum and steel with an IMP thickness of few micrometers and sufficient properties. The mechanical properties hybrid butt joints produced by the CMT-joining process in voestalpine special welding geometry have been characterized and described by using tensile tests and microhardness tests. The following conclusions are drawn from the results. Tensile tests (perpendicular to weld line) with online formation analyses show that the main formation takes place on the aluminum side.

Due to the material and thickness ratio between steel or CMT seam and aluminum no significant plasticization is recorded in the steel sheet and in the area of the CMT seam. All specimens failed beyond the HAZ in the aluminum which leads to the result of no impact of quality irregularities inside of the CMT to the stress behavior. The hardness of this zone varies between the hardness of the aluminum base material and the hardness of the welding zone, which is under 100 HV. Optical micrographs present a weld width of approx. 2.4 mm and a total length beginning from aluminum welding area to ending steel brazing area of approx. 7 mm. The determination of the HEZ of the weld seam shows that the thermally influenced zone lies within the weld seam and shows no significant expansion in the direction of the aluminum base material. The results of microhardness testing across the weld seam show that constant mechanical properties in the seam thickness direction can be used with regard to the modeling of the CMT seam.

In addition in this study a part-screening has been carried out in order to find suitable components for an aluminum steel component. Two different material and thickness combinations joined by the CMT technique in butt joint configuration were conducted to show the feasibility to generate an aluminum/steel tailored hybrid blank prototype. Based on the results presented in this paper, producing two different prototypes with material combination HC340LA/AA6016 and thicknesses of steel: 0.8 mm/aluminum 1.2 mm and steel: 1.75 mm/aluminum 3 mm is possible. It can be concluded that the prototypes provide a weight reduction up to 41% compared to the standard serial components made by steel. Another conclusion of this study is that forming a material combination with a non-hardenable aluminum alloy is due to restricted formability of Magnesium in the aluminum steel compound not possible. All specimens failed in the weld seam

during the forming operation. Assuming an annual production quantity of 220,000 units, an LBMK value of € 7.89/kg is calculated.

Acknowledgements. The authors would like to acknowledge Fronius and voestalpine Companies for providing and welding the tailored hybrid blanks used in this investigation.

Received on April 5, 2020

REFERENCES

1. SINGAR, O., ROLL, K., EIPPER, K., *Numerical Simulation of the CMT-Weld line of Tailored Hybrid Blanks*, Forming Technology Forum, 2013.
2. MERKLEIN, M., JOHANNES, M., LECHNER, M., KUPPERT, A., *Numerical Simulation of the CMT-Weld line of Tailored Hybrid Blanks*, Journal of Material Processing Technology, 2014, pp. 151–164.
3. GIERA, A., *Prozesstechnische Untersuchungen zum Rührreibschweißen metallischer Werkstoffe*, Dissertation, Bd.199, M. Geiger, K. Feldmann, Meisenbach Verlag, seiten 15–19, 2008.
4. MERKLEIN, M., GIERA, A., *Laser assisted Friction Stir Welding of drawable steel-aluminium tailored hybrids*, Int. J. Mater. Form., **1**, pp. 1299–1302, 2008.
5. SEEFELD, T., KREIMEYER, M., WAGNER, F., SEPOLD, G., *Laserstrahlfügen von Mischverbindungen*, Laser Anwenderforum, seiten 215–223, 2002.
6. KREIMEYER, M., *Alu und Stahl finden zueinander*, Komponenten+Systeme, ke 3672, seiten 50–51, 2005.
7. KREIMEYER, M., *Verfahrenstechnische Voraussetzungen zur Integration von Aluminium-Stahl Mischbauweisen in den Kraftfahrzeugbau*, Dissertation, Bd. Strahltechnik Band 30, F. Vollersten, BIAS, 2007.
8. RADSCHAIT, C., SUBERT, E., SEBOLD, G., *Laserstrahlfügen von Aluminium und Stahl*, ECLAT, seiten 169–176, 1996.
9. KREIMEYER, M., VOLLERSTEN, F., *Gap tolerant joining of aluminum with steel sheets using the hybrid technique*, ICALEO, pp. 947–951, 2006, doi:10.2351/1.5060796.
10. VOLLERSTEN, F., THOMY, C., *Laser-MIG hybrid welding of aluminium and steel- effect of process parameters on joint properties*, Welding in the world, pp. 124–132, 2002.
11. LAU, K., *Nonvakuum-Elektronenstrahlfügen von beschichteten Stahlfeinblechen und Stahl-Aluminium Mischverbindungen*, Dissertation, Bd. Berichte aus dem IW Band 02/2006, F. Bach, PZH-Verlag, 2006.
12. BACH, F., *Nonvakuum-Elektronenstrahlfügen nicht artgleicher metallischer Werkstoffe*, Endbericht der Forschungsgruppe „Hochleistungsfügetechnik für Hybridstrukturen“ FOR505, PZH- Verlag, seiten 33–64, 2009.
13. WICHART, K., IVANOVA, J., BRUCKNER, J., EINZINGER, N., FIGNER, G., LIEDL, G., BASALKA, H., LEITNER, A., *Einsatz von Bimetallen für Hybridverbindungen*, Schweiß- & Prüftechnik, Bd Sonderband, seiten 28–31, 2009.
14. SINGAR, O., MERKLEIN, M., *Study on formability characteristics of the weld seam of Aluminum Steel Tailored Hybrid Blanks*, Key Engineering Materials, **549**, pp. 302–310, 2013.
15. BRUCKNER, J., ARENHOLZ, E., *Die Stahl-Aluminium-Hybridplatine- eine innovative Lösung für den Mischbau*, DVS, seiten 335–337, 2011.
16. AGUDO, L., WEBER, S., LEITNER, A., ARENHOLZ, E., BRUCKNER, J., HACKL, H., PYZALLA, A., *Influence of Filler Composition on the Microstructure and Mechanical Properties of Steel-Aluminum Joints Produced by Metal Arc Joining*, Advanced Engineering Material, **11**, 5, pp. 350–358, 2009, doi: 10.1002/adem.200800319.